A Journal of the Gesellschaft Deutscher Chemiker

Angewandte International Edition GDCh Chemie

www.angewandte.org

Accepted Article

Title: Ultrahigh Supramolecular Cascaded Room-Temperature Phosphorescence Capturing System

Authors: Yu Liu, Man Huo, and Xian-Yin Dai

To be cited as: *Angew. Chem. Int. Ed.* 10.1002/anie.202113577

Link to VoR: https://doi.org/10.1002/anie.202113577

WILEY-VCH

10.1002/anie.202113577

WILEY-VCH

RESEARCH ARTICLE

Ultrahigh Supramolecular Cascaded Room-Temperature Phosphorescence Capturing System

Man Huo[+], Xian-Yin Dai[+], and Yu Liu*

Dedicated to the 100th anniversary of Chemistry at Nankai University

[*] Dr. M. Huo, X. Y. Dai, Prof. Dr. Yu Liu
College of Chemistry
State Key Laboratory of Elemento-Organic Chemistry
Nankai University, Tianjin 300071, P. R. China
E-mail: yuliu@nankai.edu.cn
[+] These authors contributed equally to this work.

Abstract: An ultrahigh supramolecular cascaded phosphorescence-capturing aggregate was constructed by multivalent co-assembly strategy utilizing cucurbit[7]uril (CB[7]) and amphipathic sulfonatocalix[4]arene (SC4AD). The initial dibromophthalimide derivative (G) generated a weak phosphorescent emission at 505 nm by host-guest interaction with CB[7], which further assembled with SC4AD to form homogeneously spherical nanoparticles with the dramatical enhancement of both phosphorescence lifetime to 1.13 ms and emission intensity by 40-fold. Notably, such G⊂CB[7]@SC4AD aggregate exhibited efficient phosphoresce energy transfer to Rhodamine B (RhB) or benzothiadiazole (DBT) with high efficiency (Φ_{ET}) of 84.4 % and 76.3 % and antenna effect (AE) of 289.4 and 119.5, and then each of which can function as a bridge to further transfer their energy to second near-infrared acceptor Cy5 or Nile blue (NiB) to achieve the cascaded phosphorescence energy transfer. The final aggregate with long-range effect from 425 nm to 800 nm and long-lived photoluminescence was further employed as imaging agent for multicolour cell labelling.

Introduction

Purely organic room-temperature phosphorescence (RTP) has aroused an extensive research upsurge due to its unique characteristics such as long emission lifetime, large stokes shift and high reliability working in complicated biological environments[1], which endowed RTP materials with promising potentials in the organic light-emitting diodes[2], information confidentiality and anti-counterfeiting[3], biological imaging[4] and so forth. Recently, RTP system in solution phase is an emerging research hotspot because of their time-resolved feature which can effectually eliminate autofluorescence or background fluorescence interference from tissues or cellular bio species[5]. However, the development of such system was heavily impeded as a result of the intense quenching effect of solution on excited triplet state of phosphors[6]. Although conventional strategies like crystallization[7], polymerization[8], doping[9] and matrix rigidification[10] have been exploited to construct various emissive phosphorescent systems, supramolecular methodology based on host-guest complexation is regarded as an alternative or even powerful method to realize high-efficiency RTP especially in aqueous media[11]. Macrocyclic compounds as cyclodextrins (CDs)[12] and cucurbiturils (CBs)[13] with stiff and hydrophobic cavities and stable configuration can create minimized microenvironment for molecular vibrational dissipation, suppress the nonradiative relaxation decay of excited triplet state and protect the phosphors against quenching by water, which greatly expanded the RTP materials application scope especially in complexed biosystems. Additionally, assembling-induced emission through supramolecular dynamic assembling means is also an applicable strategy to achieve significantly enhanced emission, which was applied in kinds of luminescent supramolecular systems including purely organic RTP materials[14].

Light-harvesting was perceived as imitation of photosynthesis in natural for efficiently converting light energy into chemical energy[15]. However, the natural light-harvesting systems with favourable efficiency are usually composed of multiple chromophores for multi-step sequential energy transfer process instead of the single-step energy transfer. Two-step FRET possess higher long-range energy transfer course from initial donor to final acceptor even in the absence of any spectral overlap between them so as to realize larger Stokes shift and better fluorescence detection sensitivity for final acceptor, which has been successfully utilized for photochemical catalysis[16], white light-emitting materials[17], as well as fluorescent ink for security printing[18]. Supramolecular assembly has been confirmed that it is a powerful and convenient way to build light-harvesting systems via noncovalent interaction without multiple synthesis[19]. Compared to the fluorescence-based energy transfer, the phosphorescence-based ones endow the organic dyes with a longer lifetime via an efficient triplet to singlet Förster resonance energy transfer (TS-FRET)[20]. However, the fabrication of RTP energy transfer system in aqueous phase has still faced a grand difficulty since the fast release of energy from the active donor with excited state lifetime will lead to an instantaneous increase in energy density, which is hard to be harvested by acceptor molecules because phosphorescence energy transfer needs to undergo ISC process[21]. Recently, George et al. reported a highly effective room temperature phosphorescence in solution and hydrogels via fixing the phthalimide phosphor on the supramolecular organic-inorganic hybrid which was further employed as a light-harvesting platform to realize delayed fluorescence[22]. Nevertheless, there is no report on purely organic room-temperature phosphorescence-capturing system with two-step sequential energy transfer in aqueous environment, where it remains a formidable challenge at present.

10.1002/anie.202113577

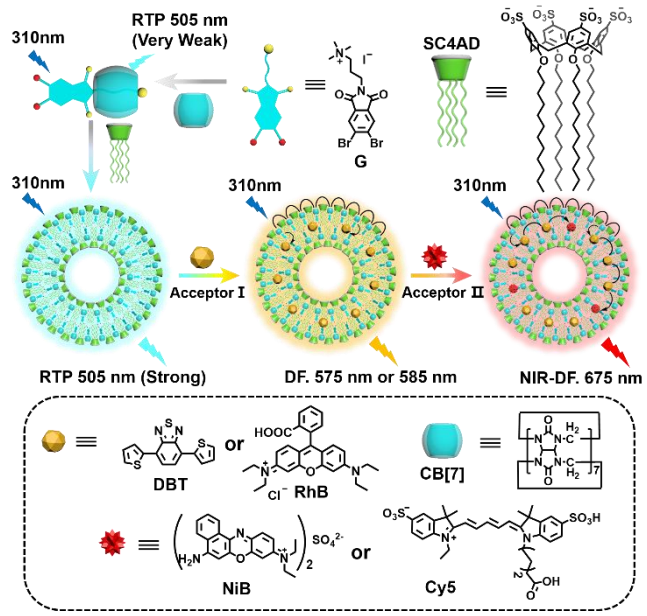

Scheme 1. Construction of the multivalent supramolecular aggregate for cascaded purely organic room-temperature phosphorescence capturing system with delayed NIR emission in aqueous solution.

Herein, we report the first example of highly efficient cascaded phosphorescence capturing system featuring long-range and long-lived emission especially delayed NIR emission via multivalent assembly approach by employing CB[7] and lower-rim dodecyl-modified sulfonatocalix[4]arene (SC4AD) (Scheme 1). Quaternary ammonium salt-substituted dibromo phthalimide derivative (G) was encapsulated by the cavity of CB[7] accompanied by the arousal of very dim RTP emission at 505 nm in aqueous solution. Furthermore, the resultant G ⊂ CB[7] complexes assembled with SC4AD to form multivalent assembly G⊂CB[7]@SC4AD which displayed spherical nanoparticles with size of around 80 nm, whose phosphorescence emission intensity was increased by 40-fold and lifetime extended to 1.13 ms which was about 52.4 times than that of G⊂CB[7]. This phenomenon is mainly because the close-packed structure formed by co-assembly with amphiphilic SC4AD immobilized the phosphors to restrict the nonradiative relaxation pathways and shielded them from quenchers to some extent. In view of the excellent phosphorescent emissive performance of G⊂CB[7]@SC4AD, we expected that the unique aggregate could serve as a light-harvesting scaffold to achieve cascaded phosphorescence energy transfer with long-range and long-lived fluorescence emission. RhB and DBT were employed as acceptors for first-step energy transfer benefiting from the good overlap between the emission band of the G⊂CB[7]@SC4AD assembly and the absorption band of RhB or DBT. Based on this, they could be successfully entrapped into the hydrophobic layer of G ⊂ CB[7]@SC4AD aggregate via the noncovalent interaction, and then an efficient one-step energy-transfer process could occur from G⊂CB[7]@SC4AD to RhB or DBT with high Φ_{ET} of 84.4 % and 76.3 % and ultrahigh AE of 289.4 and 119.5. Furthermore, the cascaded energy-transfer systems were successfully achieved by the simultaneous encapsulation of another elaborately selected NIR organic dyes Cy5 and NiB as the second energy acceptor. Overall, this two-step energy-transfer process could initially occur from G⊂CB[7]@SC4AD aggregate to RhB or DBT and then to Cy5 or NiB at a high Φ_{ET} and donor/acceptor ratio (G⊂CB[7]@SC4AD:RhB:Cy5 = 1500:12:5, Φ_{ET} = 54.0 %, AE = 190.6; G⊂CB[7]@SC4AD:RhB:NiB = 1500:12:4, Φ_{ET} = 60.5 %, AE = 97.0; G⊂CB[7]@SC4AD:DBT:Cy5 = 1500:30:6, Φ_{ET} = 58.9 %, AE = 116.8; G⊂CB[7]@SC4AD:DBT:NiB = 1500:30:5, Φ_{ET} = 74.1 %, AE = 46.2).

Results and Discussion

Seeking suitable phosphorescent molecule as a donor to perform cascaded energy transfer is the key problem that need to be addressed first. Inspired by George et al. recent work[22,23], we borrowed the corresponding excellent properties of phthalimide phosphor. The guest G was successfully synthesized through two simple steps (Scheme S1) and characterized by ^{1}H NMR spectroscopies and HR-MS (Figure S1-S3). The design of three carbons-alkyl chain of G provided it with greater hydrophobicity to anticipate better assembly with amphiphilic molecule. It is well documented that CB[7] with a robust cavity has high affinity with organic cations[24]. In this system, CB[7] could complex with G to form a stable host-guest inclusion complex G⊂CB[7] through hydrophobic interaction, hydrogen bonding and cation-dipole interactions. Firstly, we studied the host-guest binding behaviour between G and CB[7] by ^{1}H NMR spectroscopic experiments. The protons of the alkyl chain moiety (H_2, H_3, H_4) of G underwent upfield shifts, whereas other protons of G (H_1, H_5) shifted downfield (Figure S4). The binding constant (K_S) was determined to be 3.85 × 10^5 through ^{1}H NMR titration via using the nonlinear least-squares fitting method (Figure S5). due to the shielding effect of CB[7] hydrophobic cavity, while the protons of the phenyl (H_5) showed down-field shift, suggesting that the alkyl chain moiety threaded into the cavity of CB[7]. Furthermore, high-resolution mass spectrometry (HR-MS) was conducted, which showed that the intense peak of $[M\text{-}I^-]^+$ (m/z 1567.3067) fitted well the calculated value (1567.3052) substantiating a 1:1 stoichiometry between CB[7] and G (Figure S6). G and G⊂CB[7] displayed the absorption at around 310 nm in the UV-vis absorption spectra (Figure S7). The phosphorescence spectrum of G⊂CB[7] showed an emission band centered at 505 nm, which increased after vacuum degassing of the solution (Figure S8). The emission intensity of G significantly increased when the temperature decreased to 77 K thus ruling out the possibility of thermally activated delayed fluorescence (Figure S9). Then the lifetime of the emerged emission peak at 505 nm was determined to be 22.0 μs by the time-resolved PL decay curves, and it increased to 75.9 μs after vacuum degassing own to its suppressing the triplet-state excitons from being quenched (Figure S10, 11).

Furthermore, we investigated the effect of the G⊂CB[7] after co-assembly with SC4AD on phosphorescence emission behaviour. It has been well-established that amphiphilic SC4AD exhibited markedly superiority in self-assembly because its upper and lower ports were decorated with hydrophilic groups and hydrophobic groups respectively, which was constantly used to construct supramolecular emissive assemblies own to this inherent amphiphilicity[25]. As shown in Figure 1a (inset), free G displayed negligible phosphorescence and G⊂CB[7] solution also showed quite dim phosphorescence. It could be seen from Figure 1a that the phosphorescence emission of G ⊂ CB[7]@SC4AD at 505 nm significantly enhanced by about 40-fold,

10.1002/anie.202113577

indicating that the co-assembly process take place between G⊂CB[7] and SC4AD. Moreover, the phosphorescence lifetime of G⊂CB[7]@SC4AD was determined as τ = 1130.4 μs by time-resolved PL decay curve about 52.4 times longer than before, which was an order of magnitude transition from microseconds to milliseconds (Figure 1b). These results indicated that the co-assembly with SC4AD can significantly improve the phosphorescence behaviour of G⊂CB[7], which was mainly because that formed G⊂CB[7]@SC4AD aggregates have hydrophobic regions and tight close-packed structures which would greatly restrict the intramolecular rotation of G and further successfully overcome the vibrational dissipation as well as hinder triplet state from being quenched by water or dissolved oxygen thus achieving enhancement of phosphorescence emission in aqueous solution. In contrast experiments, the time-delay photoluminescence spectrum of G/SC4AD was silent under the same experimental set-up conditions (Figure S12), indicating that the CB[7] played a vital role in promoting intersystem crossing (ISC) from singlet to triplet state of G. Moreover, the stepwise introduction of SC4A without modified dodecyl chain into G⊂CB[7] solution would cause phosphorescence quenching at 505 nm (Figure S13), and the emission was almost constant upon addition of same equivalent SDBS (Figure S14), which implied that none of them could produce a marked effect of minimizing in vibrational dissipation as SC4AD to enhanced phosphorescent emission. Therefore, the unique cyclic structure and inherent amphiphilicity of SC4AD play crucial roles towards the co-assembly process with G⊂CB[7] for enhanced RTP emission.

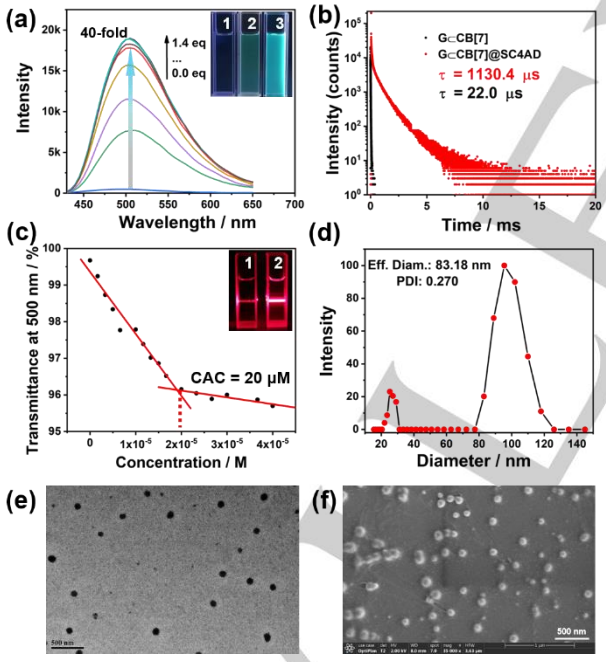

Figure 1. (a) Phosphorescence emission spectra (delayed 50 μs) of G⊂CB[7] ([G] = [CB[7]] = 2.5 × 10^{-5} M) upon the addition of 0, 0.5, 1.0, 1.5, 2.0, 2.5, 3.0, 3.5 × 10^{-5} M SC4AD in aqueous solution. Inset: photographs of solutions of G (1). G⊂CB[7] (2) and G⊂CB[7]@SC4AD (3) under 320 nm light under ambient condition. (b) Time-resolved PL decay curves of G⊂CB[7], G⊂CB[7]@SC4AD at 505 nm in aqueous solution at 298 K ([G⊂CB[7]] = 2.5 × 10^{-5} M, [SC4AD] = 2.5 × 10^{-5} M). (c) Dependence of optical transmittance at 505 nm on SC4AD concentration at a G⊂CB[7] concentration of 2.5 × 10^{-5} M. Inset: the Tyndall effect of G⊂CB[7] (1) and G⊂CB[7]@SC4AD (2) ([G] = [CB[7]] = 2.5 × 10^{-5} M, [SC4AD] = 2.5 × 10^{-5} M). (d) DLS data, (e) TEM image and (f) SEM image of G⊂CB[7]@SC4AD multivalent aggregate ([G] = 2.5 × 10^{-5}, [CB[7]] = 2.5 × 10^{-5}, [SC4AD]= 2.5 × 10^{-5}).

Next, to gain more insights for the assembly process between G⊂CB[7] and SC4AD, optical transmittance was first studied. Initially, the changes of transmittance were tested with the addition of SC4AD by fixing the concentration of G⊂CB[7] (Figure S15). The critical aggregation concentration (CAC) was determined as 20 μM according to the transmittance changes at 505 nm (Figure 1c). Meanwhile, notable opalescence under ambient light could be observed and there was obvious Tyndall effects of G⊂CB[7]@SC4AD, while there was slightly Tyndall effect for the freshly prepared G⊂CB[7] solution, suggesting the formation of the G⊂CB[7]@SC4AD aggregate (Figure 1c (inset)). Furthermore, the size and morphology of G⊂CB[7]@SC4AD were studied by dynamic light scattering (DLS), transmission electron microscope (TEM) and scanning electron microscopy (SEM) measurements. DLS experiment revealed that the average hydrodynamic diameter of G⊂CB[7]@SC4AD was 83.18 nm (Figure 1d). TEM and SEM provided visual information of G⊂CB[7]@SC4AD assembly. The image of TEM displayed some dark spherical nanoparticles (Figure 1e) with similar diameters ca.80 nm and SEM image showed analogous morphology results (Figure 1f).

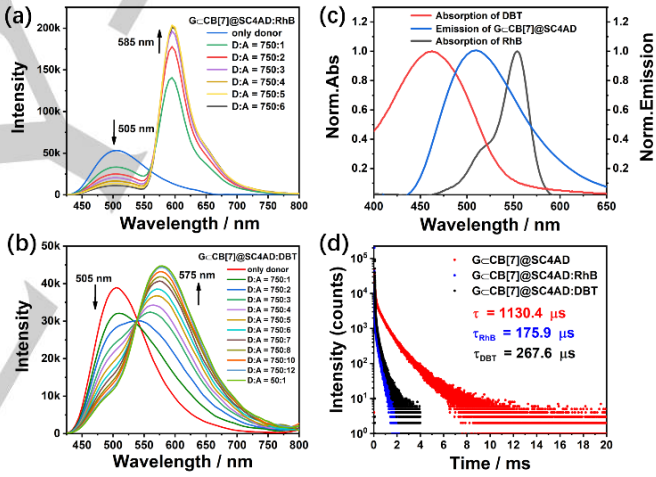

Figure 2. Phosphorescence emission spectra (delayed 50 μs) of (a) G⊂CB[7]@SC4AD:RhB, (b) G⊂CB[7]@SC4AD:DBT at different donor/acceptor ratios in aqueous solution at 298 K ([G⊂CB[7]] = 2.5 × 10^{-5} M, [SC4AD] = 2.5 × 10^{-5} M, λ_{ex} = 310 nm, 298 K). (c) Normalized emission spectrum of G⊂CB[7]@SC4AD assembly and absorption spectra of DBT, RhB. (d) Time-resolved PL decay curves of G⊂CB[7]@SC4AD, G⊂CB[7]@SC4AD:RhB, G⊂CB[7]@SC4AD:DBT at 505 nm in aqueous solution at 298 K ([G⊂CB[7]] = 2.5 × 10^{-5} M, [SC4AD] = 2.5 × 10^{-5} M, [RhB] = 2.0 × 10^{-7} M, [DBT] = 5.0 × 10^{-7} M).

TS-FRET has attracted extensive attention lately as strategy to get effective long-lived fluorescence emission[20]. However, the construction of cascaded phosphorescent capture system is a still difficult task. We chose blue phosphorescent molecules as energy donors to build a two-step sequential phosphorescent capture system, which can realize adjustable wide range and long-lived fluorescence emission through delayed sensitization process. In view of the improved phosphorescence performance of this G⊂CB[7]@SC4AD, we expected that this G⊂CB[7]@SC4AD aggregate could act as an ideal donor to establish the phosphorescence capturing scaffold in aqueous solution. RhB and DBT, two kinds of fluorescent dyes with high fluorescence

10.1002/anie.202113577

quantum yield, were selected as acceptors own to the following merits: On the one hand, their absorption band of each had an effective overlap with the emission of the G⊂CB[7]@SC4AD assembly (Figure 2c). On the other hand, the fluorescent dyes could be easily encapsulated into the close-packed structure of the obtained G⊂CB[7]@SC4AD aggregate via hydrophobic effect, which satisfied the short distance between donor and acceptor. As depicted in Figure 2a, upon the stepwise addition of RhB, the phosphorescence intensity of G⊂CB[7]@SC4AD at 505 nm decreased gradually, while the emission at 585 nm increased. The emission intensity of donor or acceptor nearly did not change until the ratio of donor and receptor was 750:6. Another evidence for efficient TS-FRET was the changes of the time-resolved PL decay curves before and after energy transfer. As shown in Figure 2d, the lifetime for G⊂CB[7]@SC4AD:RhB at 505 nm was reduced to 175.9 μs at the donor/acceptor ratio of 750:6. Such decrease was consistent with the phosphorescence energy transfer from triplet of donor to singlet of acceptor. The RhB emission at 585 nm in the G⊂CB[7]@SC4AD:RhB system was in accordance with the fluorescence of RhB, indicating the characteristic delayed-fluorescence (DF) (Figure S16). The lifetime for this DF emission at 585 nm was 179.5 μs, while the lifetime of free RhB was measured as 3.2 ns (Figure S17-S19). Φ_{ET} and AE were two important criteria to quantitatively evaluate the efficiency of this phosphorescence-capturing system. According to the deceased donor lifetime data, the value of Φ_{ET} was determined as 84.4% at the donor/acceptor ratio of 750:6 (Figure 2d, Figure S36). The AE was calculated to be 289.4 at same donor/acceptor ratio (Figure S42).

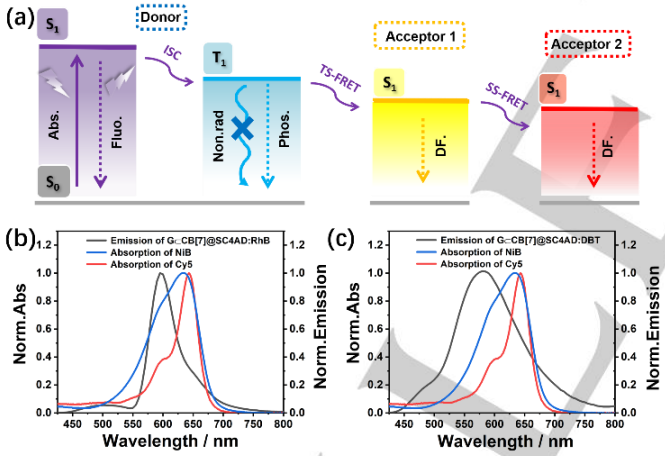

Figure 3. Simplified Jablonski diagram to explain the possible mechanism for cascaded phosphorescence-capturing process in the present case. (Abs. = absorption, Fluo. = fluorescence, DF. = delayed fluorescence, Non. rad. = non-radiation, ISC = intersystem crossing, Phos. = Phosphorescence, TS-FRET = Triplet to singlet Förster resonance energy transfer, SS-FRET = Singlet to singlet Förster resonance energy transfer. Normalized emission spectrum of G⊂CB[7]@SC4AD:RhB assembly (b), G⊂CB[7]@SC4AD:DBT assembly (c) and absorption spectra of DBT, RhB.

Moreover, we substituted the above acceptor RhB with DBT to verify the universality of the G⊂CB[7]@SC4AD as phosphorescence-capturing platform. As shown in Figure 2b, with gradually addition of DBT into G⊂CB[7]@SC4AD assembly solution, the phosphorescence intensity of donor at 505 nm decreased and the emission at 575 nm increased greatly. The lifetime for G⊂CB[7]@SC4AD:DBT at 505 nm decreased to 267.6 μs at the donor/acceptor ratio of 50:1 (Figure 2d), which was corresponding to the TS-FRET process. The DBT emission at 575 nm in the G⊂CB[7]@SC4AD:DBT system was identical with the fluorescence of DBT, suggesting its delayed-fluorescence (Figure S20). The lifetime for this DF emission at 575 nm was measured to be 214.7 μs, whereas the lifetime for DBT alone was tested as 9.7 ns (Figure S19, S21, S22). In addition, the value of Φ_{ET} was determined as 76.3% at the donor/acceptor ratio of 50:1 according to the deceased donor lifetime data (Figure 2d, Figure S37) and the AE was 119.5 at same donor/acceptor ratio (Figure S43). In control experiments, the emission of G⊂CB[7]:RhB and G⊂CB[7]:DBT at 585 nm were all invalid, suggesting that phosphorescence energy transfer between G⊂CB[7] and fluorescent dye (RhB or DBT) was ascribed to the multivalent assembly with SC4AD (Figure S23). The UV absorption of RhB and DBT under the experimental concentration was almost negligible, indicating that 310-nm excitation predominantly excited the primary phthalimide donor (Figure S24a, b). Furthermore, both G-free assembly of RhB and DBT displayed negligible delayed fluorescence emission when excited at 310 nm, whereas dramatic delayed fluorescence emission could be observed in G⊂CB[7]@SC4AD:RhB and G⊂CB[7]@SC4AD:DBT under the same experimental conditions, indicative of the valid phosphorescence energy transfer from donor to acceptor (Figure S25a,b).

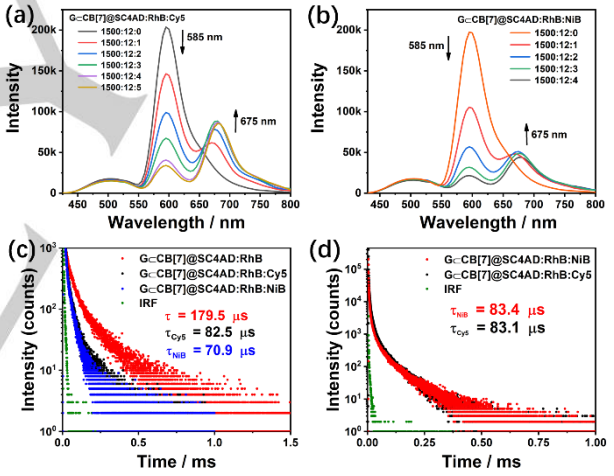

Figure 4. Phosphorescence emission spectra (delayed 50 μs) of (a) G⊂CB[7]@SC4AD:RhB:Cy5, (b) G⊂CB[7]@SC4AD:RhB:NiB at different donor/acceptor ratios in aqueous solution at 298 K. Time-resolved PL decay curves of G⊂CB[7]@SC4AD :RhB, G⊂CB[7]@SC4AD:RhB:Cy5, G⊂CB[7]@SC4AD:RhB:NiB at 585 nm (c), at 675 nm (d) in aqueous solution at 298 K ([G⊂CB[7]] = 2.5 × 10^{-5} M, [SC4AD] = 2.5 × 10^{-5} M, [RhB] = 2.0 × 10^{-7} M, [Cy5] = 8.3 × 10^{-8} M, [NiB] = 6.7 × 10^{-8} M). IRF = Instrument response function.

Considering that the photosynthetic light harvesting system in nature is composed of multiple polychromatic components for multi-step sequential energy transfer, rather than simple one-step energy transfer, we further explored the possibility of cascade energy transfer process of the resultant supramolecular aggregate G⊂CB[7]@SC4AD:RhB, G⊂CB[7]@SC4AD:DBT. NiB and Cy5 were two organic dyes with NIR emission, the absorption band of which possessed the good spectral overlaps with the emission band of G⊂CB[7]@SC4AD:RhB, and in the same way overlapped well with emission band of G⊂CB[7]@SC4AD:DBT (Figure 3b, 3c). We first investigated G⊂

10.1002/anie.202113577

CB[7]@SC4AD:RhB system as the donor for second-step energy transfer. When the second acceptor Cy5 was introduced into the G⊂CB[7]@SC4AD:RhB system, the DF emission of RhB at 585 nm decreased and a new emission band at 675 assigned as Cy5 appeared, indicating that the energy transfer happened from the singlet of RhB to singlet of Cy5 (Figure 4a). More critically, the emission intensity at 505 nm remain almost unchanged in this process, which implied that there was little energy transfer from the G⊂CB[7]@SC4AD assembly to the secondary receptor Cy5. There were two possible reasons: On the one hand, primary energy transfer from G⊂CB[7]@SC4AD to RhB possessed high energy transfer efficiency and the phosphorescence emission of G⊂CB[7]@SC4AD at 505 nm was greatly quenched. On the other hand, the absorption spectrum of secondary acceptor Cy5 and G⊂CB[7]@SC4AD system only overlapped with a slight extent, but overlapped to a large extent with RhB. In another experiment, there was a little emission of Cy5 at 675 nm with addition of Cy5 into the G⊂CB[7]@SC4AD system, indicating there was no effective energy transfer between them (Figure S26). Therefore, RhB served as a vital link to achieve the cascade phosphorescence-capturing profiting from its ideal absorption and emission properties in this system. According to the time-resolved PL decay curves (Figure 4c), the lifetime of G ⊂ CB[7]@SC4AD:RhB:Cy5 at 585 nm abated to 82.5 μs. And the lifetime at 675 nm ascribed to Cy5 was 83.1 μs (Figure 4d, Figure S27a) while the lifetime for Cy5 alone was measured as 2.0 ns (Figure S28), indicative of the long-lived NIR emission. In addition, the emission of Cy5 in the G⊂CB[7]@SC4AD:RhB:Cy5 system coincided with the fluorescence emission of free Cy5, representing the characteristic delayed-fluorescence (DF) (Figure S29). It was worth mentioning that the emission of primary and secondary receptors was delayed fluorescence with microsecond lifetime through two-step energy transfer process of TS-FRST and SS-FRET, and the possible mechanism of cascaded phosphorescence-capturing system was shown in Figure 3a. Therefore, such cascaded phosphorescence-capturing was an efficient strategy to obtain the long-range and long-lived tunable fluorescence including NIR emission. In this system, the value of Φ_{ET} was calculated to be 54.0 % according to the lifetime of donor with a molar ratio of G ⊂ CB[7]@SC4AD to RhB to Cy5 of 1500:12:5 (Figure 4c, Figure S38). The AE was 190.6 at above high ratio (Figure S44).

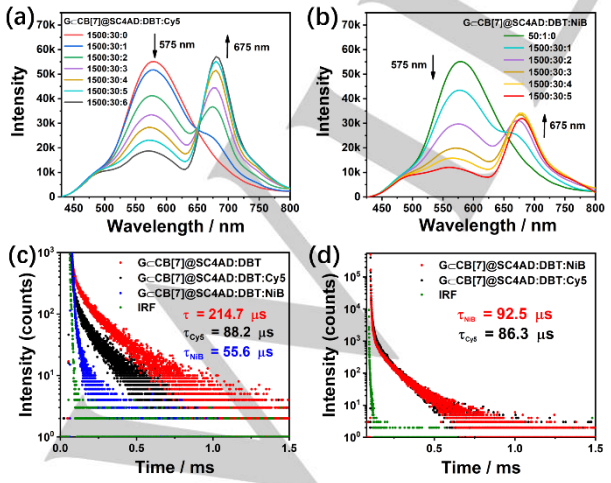

Figure 5. Phosphorescence emission spectra (delayed 50 μs) of (a) G⊂CB[7]@SC4AD:DBT:Cy5, (b) G ⊂ CB[7]@SC4AD:DBT:NiB at different donor/acceptor ratios in aqueous solution at 298 K. Time-resolved PL decay curves of G ⊂ CB[7]@SC4AD :DBT, G ⊂ CB[7]@SC4AD:DBT:Cy5, G ⊂ CB[7]@SC4AD:DBT:NiB at 575 nm (c), at 675 nm (d) in aqueous solution at 298 K ([G⊂CB[7]] = 2.5 × 10^{-5} M, [SC4AD] = 2.5 × 10^{-5} M, [DBT] = 5.0 × 10^{-7} M, [Cy5] = 1.0 × 10^{-7} M, [NiB] = 8.3 × 10^{-8} M). IRF = Instrument response function.

NiB, as another secondary receptor, was also introduced into the G ⊂ CB[7]@SC4AD:RhB system to study the secondary energy transfer performance. As shown in Figure 4c, upon the stepwise addition of NiB, the DF emission at 585 nm gradually decreased and the DF emission of NiB was observed (Figure S30). Similarly, the emission band at 505 kept unchanged during this process, indicating that NiB was also an appropriate secondary acceptor for the G⊂CB[7]@SC4AD:RhB assembly. In control experiment, when added NiB into the G⊂CB[7]@SC4AD system, there was no significant increase of the emission of NiB at 675 nm, implying that effective energy transfer could not take place between them (Figure S31). The lifetime of G ⊂ CB[7]@SC4AD:RhB:NiB at 585 was declined to 70.9 μs (Figure 4c), and the lifetime at 675 nm belonging to NiB was 83.4 μs (Figure 4d, Figure S27b). The lifetime of NiB was tested as 1.8 ns (Figure S32). Additionally, the value of Φ_{ET} was 60.5 % according to the change of lifetime at 585 nm and the AE was 97.0 at the molar ratio of G⊂CB[7]@SC4AD to RhB to NiB of 1500:12:4 (Figure 4c, Figure S39, 45).

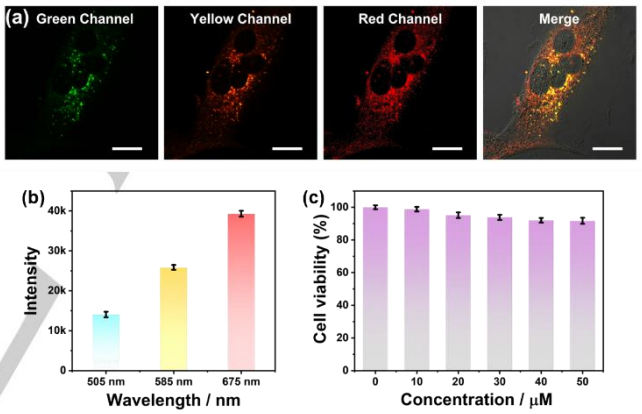

Figure 6. Confocal microscopy images of A549 cells co-stained with **G** ⊂ CB[7]@SC4AD:RhB:Cy5 ([**G**⊂CB[7]] = 2.5 × 10^{-5} M, [SC4AD] = 2.5 × 10^{-5} M, [RhB] = 2.0 × 10^{-7} M, [Cy5] = 8.3 × 10^{-8} M). For Green Channel, λ_{ex} = 405 nm, λ_{em} = 450-550 nm. For Yellow Channel, λ_{ex} = 405 nm, λ_{em} = 550-650 nm. For Red Channel, λ_{ex} = 405 nm, λ_{em} = 650-750 nm. (b) Time-resolved fluorescence (TRF) signal respectively detected at 505 nm, 585 nm and 675 nm via microplate reader. (c) Cell viability of A549 cells for G ⊂ CB[7]@SC4AD:RhB:Cy5 at different concentration.

On the base of above, Cy5 and NiB as secondary receptor, were also separately investigated for sequential phosphorescence energy transfer of G⊂CB[7]@SC4AD:DBT. As shown in Figure 5a and 5b, the DBT intensity was quenched with the DF emission at 675 nm gradually emerging upon titration of dyes (Figure S33, 34). The lifetimes at 575 nm were decreased to 88.2 μs for G⊂CB[7]@SC4AD:DBT:Cy5 and 55.6 μs for G⊂CB[7]@SC4AD:DBT:NiB (Figure 5c), demonstrating the effective cascaded phosphorescence transfer for G⊂CB[7]@SC4AD:DBT system. The lifetime were determined to be as 86.3 μs of Cy5 at 675 nm in G⊂CB[7]@SC4AD:DBT:Cy5 system, and 92.5 μs of NiB at 675 nm in G⊂CB[7]@SC4AD:DBT:NiB system (Figure 5d, Figure S35). The value of Φ_{ET} and AE were calculated as 58.9 % and 116.8 at the ratio of 1500:30:6 for G ⊂

CB[7]@SC4AD:DBT:Cy5 (Figure 5c, Figure S40, 46). And the value of Φ_{ET} and AE were acquired as 74.1 % and 46.2 at the ratio of 1500:30:5 for G⊂CB[7]@SC4AD:DBT:NiB (Figure 5c, Figure S41, 47). The UV absorption of Cy5 and NiB was little (Figure S24c, d), and there were no perceptible delayed fluorescence emission for DBT@CB[7]@SC4AD, Cy5@CB[7]@SC4AD when excited at 310 nm (Figure S25c,d). These results jointly validated the encapsulation of fluorescent dyes RhB or DBT and Cy5 or NiB into the G⊂CB[7]@SC4AD aggregate as well as the sequential energy transfer in the relay mode.

Additionally, in consideration of its excellent Φ_{ET} and high AE value, we investigated the possibility of G ⊂ CB[7]@SC4AD:RhB:Cy5 as an imaging agent for multicolour cell labelling. Firstly, the cytotoxicity of above system was examined by using human lung adenocarcinoma cells (A549 cancer cells) as model. Standard cell counting kit-8 (CCK-8) analysis revealed that this system displayed negligible toxicity with the cell survival rate greater than 92% under increasing concentration to 50 μM (Figure 6c). Next, confocal laser scanning microscopy (CLSM) was carried out to explore its feasibility as cell labelling agent. As depicted in Figure 6a, three channels together exhibited the related fluorescence signal especially near-infrared emission which covered almost the whole visible spectrum. We further investigated the subcellular distribution of such obtained supramolecular aggregate by co-staining with a commercial lysosome dye Lyso-Tracker Green. Notably, the red emission signal assigned to aggregate displayed favourable overlap with the green region of Lyso-Tracker Green with a high Pearson correlation coefficient as 0.80, implying the specific distribution of such aggregate in lysosomes. Moreover, the intensity profiles of Lyso-Tracker Green and the red emission signal in co-staining image also showed a good synchronization from the ROI (linear regions of interest) analysis, which further illustrated the lysosome-targeting ability of such aggregate (Figure S48). Particularly, microplate reader was also used to quantitatively analyse the time-resolved fluorescence (TRF) signal. As shown in Figure 6b, three end points assigned to 505 nm, 585 nm and 675 nm all presented the corresponding TRF signal after a delay of 50 microseconds after incubation with cells for 12 h. These results jointly indicated that such multivalent supramolecular aggregate can not only be used as a low-toxic polychromatic cell imaging reagent, but also as a long-range time-resolved fluorescent marker to avoid the interference of background fluorescence signals, which has potential applications in the field of multicolour cell imaging and labelling.

Conclusion

In conclusion, we have constructed the first example of purely organic room-temperature phosphorescence-capturing system with two-step cascaded phosphorescence energy transfer based on the multivalent supramolecular aggregate of CB[7] and SC4AD, which is capable of emitting long-range and long-lived fluorescence ranging from 425-800 nm even including NIR delayed fluorescence at 675 nm in aqueous media and successfully being applied to multicolour cell labelling imaging. Host-induced phosphorescence emission and further assembling-enhanced emission synergistically enable this multivalent supramolecular aggregate G⊂CB[7]@SC4AD to serve as a versatile scaffold to achieve efficient cascade phosphorescence energy transfer after the successive introduction of primary (RhB or DBT) and secondary energy acceptors (Cy5 or NiB). Remarkably, the resultant aggregate with low toxicity can be further utilized as cell labelling agent for multicolour imaging. This multivalent supramolecular aggregate is expected to offer a convenient and feasible strategy for the fabrication of cascaded phosphorescence energy transfer system with long-range and long-lived photoluminescence especially NIR delayed emission, as well as bringing about new opportunities toward the design of more advanced phosphorescent supramolecular systems towards living cell imaging for biological studies.

Acknowledgements

This work was financially supported by the National Natural Science Foundation of China (grant nos. 21772099 and 21861132001). M. Huo and X.-Y. Dai contributed equally to this work. Y. Liu acquired the funding, revised the manuscript, and supervised the project.

Conflict of interest

The authors declare no conflict of interest

Keywords: multivalent supramolecular aggregate • cascaded phosphorescence energy transfer • phosphorescence-capturing system • NIR delayed emission • multicolour cell labelling

[1] a) Y. Yu, M. S. Kwon, J. Jung, Y. Zeng, M. Kim, K. Chung, J. Gierschner, J. H. Youk, S. M. Borisov, J. Kim, *Angew. Chem. Int. Ed.* **2017**, *56*, 16207-16211; b) G. Zhang, G. M. Palmer, M. W. Dewhirst, C. L. Fraser, *Nat. Mater.* **2009**, *8*, 747-751. c) S. Kuila, K. V. Rao, S. Garain, P. K. Samanta, S. Das, S. K. Pati, M. Eswaramoorthy, S. J. George, *Angew. Chem. Int. Ed.* **2018**, *57*, 17115-17119.

[2] C. Adachi, M. A. Baldo, M. E. Thompson, S. R. Forrest, *J. Appl. Phys.* **2001,** *90*, 5048-5051.

[3] a) K. Jiang, L. Zhang, J. Lu, C. Xu, C. Cai, H. Lin, *Angew. Chem. Int. Ed.* **2016**, *55*, 7231-7235; b) S. Cai, H. Shi, D. Tian, H. Ma, Z. Cheng, Q. Wu, M. Gu, L. Huang, Z. An, Q. Peng, W. Huang, *Adv. Funct. Mater.* **2018**, *28,* 1705045; c) X. Yao, J. Wang, D. Jiao, Z. Huang, O. Mhirsi, F. Lossada, L. Chen, B. Haehnle, A. J. C. Kuehne, X. Ma, H. Tian, A. Walther, *Adv. Mater.* **2021**, *33*, e2005973; d) L. Bian, H. Shi, X. Wang, K. Ling, H. Ma, M. Li, Z. Cheng, C. Ma, S. Cai, Q. Wu, N. Gan, X. Xu, Z. An, W. Huang, *J. Am. Chem. Soc.* **2018**, *140*, 10734-10739.

[4] a) J. Yang, M. Fang, Z. Li, *Acc. Mater. Res.* **2021**, *2*, 644-654. b) S. Zhang, M. Hosaka, T. Yoshihara, K. Negishi, Y. Iida, S. Tobita, T. Takeuchi, *Cancer Res* **2010**, *70*, 4490-4498. c) X. F. Wang, H. Xiao, P. Z. Chen, Q. Z. Yang, B. Chen, C. H. Tung, Y. Z. Chen, L. Z. Wu, *J. Am. Chem. Soc.* **2019,** *141*, 5045-5050.

[5] a) Y. Wang, H. Gao, J. Yang, M. Fang, D. Ding, B. Z. Tang, Z. Li, *Adv. Mater.* **2021**, *33*, e2007811; b) J. Yang, Y. Zhang, X. Wu, W. Dai, D. Chen, J. Shi, B. Tong, Q. Peng, H. Xie, Z. Cai, Y. Dong, X. Zhang, *Nat. Commun.* **2021**, *12*, 4883.

[6] a) T. Zhang, X. Ma, H. Wu, L. Zhu, Y. Zhao, H. Tian, *Angew. Chem. Int. Ed.* **2020**, *59*, 11206-11216. b) H. Zhu, I. Badia-Dominguez, B. Shi, Q. Li, P. Wei, H. Xing, M. C. Ruiz Delgado, F. Huang, *J. Am. Chem. Soc.* **2021,** *143*, 2164-2169.

[7] a) Y. Gong, G. Chen, Q. Peng, W. Z. Yuan, Y. Xie, S. Li, Y. Zhang, B. Z. Tang, *Adv. Mater.* **2015**, *27*, 6195-6201; b) J. Yang, X. Zhen, B. Wang, X. Gao, Z. Ren, J. Wang, Y. Xie, J. Li, Q. Peng, K. Pu, Z. Li, *Nat. Commun.* **2018**, *9*, 840; c) B. Zhou, G. Xiao, D. Yan, *Adv. Mater.* **2021,** *33*, e200757.

[8] a) L. Gu, H. Wu, H. Ma, W. Ye, W. Jia, H. Wang, H. Chen, N. Zhang, D. Wang, C. Qian, Z. An, W. Huang, Y. Zhao, *Nat. Commun.* **2020**, *11*, 944; a) Y. Su, Y. Zhang, Z. Wang, W. Gao, P. Jia, D. Zhang, C. Yang, Y. Li, Y. Zhao, *Angew. Chem. Int. Ed.* **2020**, *59*, 9967-9971; c) Z. Y. Zhang, W. W. Xu, W. S. Xu, J. Niu, X. H. Sun, Y. Liu, *Angew. Chem. Int. Ed.* **2020**, *59*, 18748-18754.

[9] a) D. Lee, O. Bolton, B. C. Kim, J. H. Youk, S. Takayama, J. Kim, *J. Am. Chem. Soc.* **2013**, *135*, 6325-6329; b) Z. Lin, R. Kabe, N. Nishimura, K. Jinnai, C. Adachi, *Adv. Mater.* **2018**, *30*, e1803713.

[10] a) S. Xu, W. Wang, H. Li, J. Zhang, R. Chen, S. Wang, C. Zheng, G. Xing, C. Song, W. Huang, *Nat. Commun.* **2020**, *11*, 4802; b) Z. A. Yan, X. Lin, S. Sun, X. Ma, H. Tian, *Angew. Chem. Int. Ed.* **2021**, *60*, 19735-19739. c) Y. Zhang, Y. Su, H. Wu, Z. Wang, C. Wang, Y. Zheng, X. Zheng, L. Gao, Q. Zhou, Y. Yang, X. Chen, C. Yang, Y. Zhao, *J. Am. Chem. Soc.* **2021,** *143,* 13675-13685.

[11] a) W. L. Zhou, Y. Chen, Q. Yu, H. Zhang, Z. X. Liu, X. Y. Dai, J. J. Li, Y. Liu, *Nat. Commun* **2020**, *11*, 4655; b) Y. Lei, W. Dai, J. Guan, S. Guo, F. Ren, Y. Zhou, J. Shi, B. Tong, Z. Cai, J. Zheng, Y. Dong, *Angew. Chem. Int. Ed.* **2020**, *59*, 16054-16060; c) P. Wei, X. Zhang, J. Liu, G. G. Shan, H. Zhang, J. Qi, W. Zhao, H. H. Sung, I. D. Williams, J. W. Y. Lam, B. Z. Tang, *Angew. Chem. Int. Ed.* **2020**, *59*, 9293-9298; d) X. Yu, W. Liang, Q. Huang, W. Wu, J. J. Chruma, C. Yang, *Chem. Commun.* **2019,** *55,* 3156-3159.

[12] D. Li, F. Lu, J. Wang, W. Hu, X. M. Cao, X. Ma, H. Tian, *J. Am. Chem. Soc.* **2018**, *140*, 1916-1923.

[13] a) X. K. Ma, W. Zhang, Z. Liu, H. Zhang, B. Zhang, Y. Liu, *Adv. Mater.* **2021**, *33*, e2007476; b) Z.-Y. Zhang, Y. Chen, Y. Liu, *Angew. Chem. Int. Ed.* **2019**, *58*, 6028-6032.

[14] a) X. Ma, J. Wang, H. Tian, *Acc. Chem. Res.* **2019**, *52*, 738-748. b) J. Wang, Z. Huang, X. Ma, H. Tian, *Angew. Chem. Int. Ed.* **2020**, *59*, 9928-9933.

[15] a) Z. Xu, S. Peng, Y. Y. Wang, J. K. Zhang, A. I. Lazar, D. S. Guo, *Adv. Mater.* **2016**, *28*, 7666-7671. b) X. Zhu, J.-X. Wang, L.-Y. Niu, Q.-Z. Yang, *Chem. Mater.* **2019**, *31*, 3573-3581; c) H. Q. Peng, L. Y. Niu, Y. Z. Chen, L. Z. Wu, C. H. Tung, Q. Z. Yang, *Chem. Rev.* **2015**, *115*, 7502-7542.

[16] a) M. Hao, G. Sun, M. Zuo, Z. Xu, Y. Chen, X. Y. Hu, L. Wang, *Angew. Chem. Int. Ed.* **2020**, *59*, 10095-10100; b) W. J. Li, X. Q. Wang, D. Y. Zhang, Y. X. Hu, W. T. Xu, L. Xu, W. Wang, H. B. Yang, *Angew. Chem. Int. Ed.* **2021**, *60*, 18761-18768.

[17] G. Sun, W. Qian, J. Jiao, T. Han, Y. Shi, X.-Y. Hu, L. Wang, *J. Mater. Chem. A* **2020**, *8*, 9590-9596.

[18] Z. Xu, D. Gonzalez-Abradelo, J. Li, C. A. Strassert, B. J. Ravoo, D.-S. Guo, *Mater. Chem. Front.* **2017**, *1*, 1847-1852.

[19] J. J. Li, Y. Chen, J. Yu, N. Cheng, Y. Liu, *Adv. Mater.* **2017**, *29*.

[20] a) S. Kuila, S. J. George, *Angew. Chem. Int. Ed.* **2020**, *59*, 9393-9397; b) H. Gui, Z. Huang, Z. Yuan, X. Ma, *CCS. Chem.* **2021**, *3*, 481-489; c) C. Fan, L. Wei, T. Niu, M. Rao, G. Cheng, J. J. Chruma, W. Wu, C. Yang, *J. Am. Chem. Soc.* **2019,** *141,* 15070; d) A. Kirch, M. Gmelch, S. Reineke, *J. Phys. Chem. Lett.* **2019**, *10*, 310-315.

[21] a) R. Gao, D. Yan, *Chem. Sci.* **2017**, *8*, 590-599; b) Z. Li, Y. Han, F. Wang, *Nat. Commun.* **2019**, *10*, 3735.

[22] S. Garain, B. C. Garain, M. Eswaramoorthy, S. K. Pati, S. J. George, *Angew. Chem. Int. Ed.* **2021**, *60*, 19720-19724.

[23] S. Garain, S. Kuila, B. C. Garain, M. Kataria, A. Borah, S. K. Pati, S. J. George, *Angew. Chem. Int. Ed.* **2021**, *60*, 12323-12327.

[24] S. J. Barrow, S. Kasera, M. J. Rowland, J. del Barrio, O. A. Scherman, *Chem. Rev.* **2015**, *115*, 12320-12406.

[25] a) P. Li, Y. Chen, Y. Liu, *Chin. Chem. Lett.* **2019**, *30*, 1190-1197; b) Y. C. Pan, X. Y. Hu, D. S. Guo, *Angew. Chem. Int. Ed.* **2021**, *60*, 2768-2794.

10.1002/anie.202113577

WILEY-VCH

RESEARCH ARTICLE

Ultrahigh Supramolecular Cascaded Room-Temperature Phosphorescence Capturing System.

Man Huo[+], Xian-Yin Dai[+], and Yu Liu*

An ultrahigh supramolecular cascaded RTP-capturing system was constructed based on multivalent supramolecular aggregate using CB[7] and SC4AD in aqueous medium, where RTP energy transfer process took place from G⊂CB[7]@SC4AD to primary (RhB or DBT) and then to secondary energy acceptors (Cy5 or NiB), thus exhibiting long-range and long-lived photoluminescence especially NIR delayed emission (675 nm).